ADSORPTIVE REMOVAL OF TANNIC ACID BY ACTIVATED CARBON FROM AQUEOUS SOLUTION

Thesis submitted in partial fulfillment of the requirement for the award of degree of

Master of Technology

in

Chemical Engineering

By

Shubhjeet Singh

M. Tech. 2nd year

(Roll No. 601011013)

UNDER THE GUIDANCE OF

Dr. J. P. Kushwaha
Assistant Professor
Department of Chemical Engineering
Thapar University, Patiala

Department of Chemical Engineering
Thapar University
Patiala-147004, Punjab

August, 2012

CERTIFICATE

This is to certify that the thesis entitled **"Adsorptive removal of tannic acid by activated carbon from aqueous solution"**, is an authentic record of my own work carried out as requirements for the award of degree of Master of Technology in Chemical Engineering from Thapar University, Patiala, under the supervision of Dr. J.P. Kushwaha, Assistant Professor, Department of Chemical Engineering, Thapar University, Patiala, during January to July 2012.

Shubhjeet Singh

Date: 20/08/2012

Shubhjeet Singh
(Roll No: 601011013)

It is certified that the above statement made by the student is correct to the best of our knowledge and belief.

20.08.12

Dr. J.P. Kushwaha
Assistant Professor
Department of Chemical Engineering
Thapar University, Patiala

Countersigned by

10.01.2013

Dr. Rajeev Mehta
Associate Professor and Head
Department of Chemical Engineering
Thapar University, Patiala

Dr. S. K. Mohapatra
Dean, Academic Affairs
Thapar University, Patiala

ABSTRACT

Tannic Acid (TA) is a specific commercial form of tannin, a type of polyphenol. Commercial TA has the formula $C_{76}H_{52}O_{46}$. TA is a constituent of natural organic matter and occurs naturally from the breakdown of plant biomass. Therefore, it is found in surface and ground water naturally. Also, it is found in industrial wastewater discharged from coir and cork process, plant medicine, paper, and leather industries. A carcinogenic disinfection by-product such as trihalomethane can form in presence of TA during chlorination process for drinking water production. In addition as a water soluble polyphenolic compound, tannic acid has toxicity for aquatic organisms such as algae, fish and invertebrates.

In this study, adsorptive removal of TA from aqueous solution on to commercial activated carbon (ACC) was evaluated. pH study showed that highest TA removal efficiency of 67.5% and 66.02% were obtained at pH_i = 2 and 3, respectively. There is no significant differences in the TA removal at pH_i = 2 and 3, therefore, pH_i = 3 was chosen as optimum pH_i ($pH_{i\text{-}opt}$) to save the acid used for pH adjustment.

Adsorbent dosage study showed that an increase in ACC dosage resulted in an increase in TA removal up to a certain value and thereafter the removal efficiency remained almost constant. An increase in the removal with the increase in m_{ad} can be attributed to greater surface area and the availability of more adsorption sites. Very minute increase in TA removal was found for $m_{ad} \geq 15$ g/l f.

Pseudo-first-order and pseudo-second-order kinetic models used to examine their validity with the experimental kinetic adsorption data and pseudo second-order kinetic model with non-linear regression best fits the adsorption kinetics.

Isothermal experiments were performed at 291, 301 and 311 K with C_0 values of 50, 100 and200 mg/l at $pH_{i\text{-}opt}$ and $m_{ad\text{-}opt}$ of ACC. Various isotherms such as Freundlich, Langmuir and Redlich-Peterson (R-P) were used to represent the adsorption equilibrium data. The TA adsorption onto ACC was found to increase with an increase in *T*. Therefore, it can

be concluded that TA adsorption onto ACC is an endothermic process. It was found that any of the isotherms can be used for isotherm modeling. But , it may be concluded that R-P isotherm generally best-fits the equilibrium adsorption of TA onto ACC at all temperatures.

Very poor desorption of TA was observed with the NaOH and ethanol and are nearly same. Acetone showed maximum desorption of TA from spent adsorbents amongst chemical desorption. Thermal desorption of TA from ACC showed maximum desorption amongst chemical and thermal desorption methods.

ACKNOWLEDGEMENT

I express my sincerest regards and gratitude to my supervisor Dr. J. P. Kushwaha, Assistant Professor, Department of Chemical Engineering, Thapar University, Patiala, for his valuable guidance and suggestions. Without his encouragement and guidance, this thesis would not have been materialized. He guided me and gave me valuable inputs to understand the minute details of each and every step, for the successful completion of thesis.

Also, I would like to thank Dr. Rajeev Mehta, Associate Professor and Head of Chemical Engineering Department, Thapar University, Patiala for his kind cooperation and encouragement which helped me in the completion of this work.

Further, I would like to thank my parents, seniors and friends for their help and support at various stages of my work.

Last but not the least, the generous support of all the staff members of Chemical Engineering Department is greatly appreciated.

Above all, I express my indebtedness to the "**ALMIGHTY**" for all his blessings and kindness.

SHUBHJEET SINGH

CONTENTS

List of Figures

List of Tables

ABBREVIATIONS

ACC	Activated Carbon
CEC	Cation Exchange Capacity
CPB	Cetylpyridinium Bromide
D/DBP	Disinfectants and Disinfection By-Products
EPA	Environmental Protection Agency
FTIR	Fourier Transform Infrared (spectroscopy)
MPSD	Marquardt's Percent Standard Deviation
NMR	Nuclear Magnetic Resonance
R-P	Redlich-Peterson
SMZ	Surfactant-Modified Zeolite
TA	Tannic Acid
XPS	X-ray Photon Spectroscopy

CHAPTER- 1

INTRODUCTION

1.1 GENERAL

Rivers, lakes and other water-bodies are being contaminated due to effluent discharge from industrial activities. The explosive population growth and expansion of urban areas has exacerbated the adverse impacts on water resources. Until 1950s, the discharging of waste in the environment was the way of eliminating them, until the auto-purifying capacity of the environment was not sufficient. The permitted levels have been vastly exceeded; causing such environmental contamination that our natural resources cannot be used for certain uses and their characteristics have been altered. The main problem stems from waste coming from industry and agriculture, despite the fact that the population also plays an important role in environmental contamination. It has now been realized that even trace quantities of organic contaminants in drinking water are hazardous, in particular aromatic and aliphatic hydrocarbons and their substituted compounds. In the present study removal of tannic acid (TA) by adsorption method onto commercial activated carbon reported.

1.2 CHARACTERISATION, USES AND TOXICITY OF TA

TA is a specific commercial form of tannin, a type of polyphenol. Commercial tannic acid has the formula $C_{76}H_{52}O_{46}$. It is an anionic organic pollutant of relatively high molecular weight (1701.2 g mol^{-1}). It is readily soluble in water and it's solubility in water is 2850 g/L. More details of properties of TA are given in Table 1.1.

Tannins are a basic ingredient in the chemical staining of wood. TA can be applied to woods low in tannin so chemical stains that require tannin content

will react. Also, TA is a common mordant used in the dyeing process for cellulose fibers such as cotton.

TA is also used as an after treatment to improve wash fastness properties of acid dyed polyamide. It is also an alternative for fluorocarbon after treatments to impart anti-staining properties to polyamide yarn or carpets. However, due to economic considerations currently the only widespread use as textile auxiliary is the use as an agent to improve chlorine fastness (i.e. resistance against dye bleaching due to cleaning with hypochlorite solutions in high-end polyamide 6,6-based carpets and swimwear). A particular and unique textile application of tannic acid is the activation of flock, which is basically an anti-static after treatment.

TA is a constituent of natural organic matter and occurs naturally from the breakdown of plant biomass. Therefore, it is found in surface and ground water naturally. Also, it is found in industrial wastewater discharged from coir and cork process, plant medicine, paper, and leather industries (Wang et al., 2011). A carcinogenic disinfection by-product such as trihalomethane can form in presence of TA during chlorination process for drinking water production (Wang et al., 2010). TA has been currently regulated by the U.S. Environmental Protection Agency (EPA) under the Stage 1 Disinfectants and Disinfection By-Products (D/DBP) Rule.

In addition as a water soluble polyphenolic compound, tannic acid has toxicity for aquatic organisms such as algae, phytoplankton, fish and invertebrates. Therefore, it is of great importance to remove tannic acid from water and wastewater in terms of protecting human health and environment.

Table 1.1. Properties of Tannic Acid

Parameters	**Tannic Acid**
Synonyms	Acidum tannicum, Gallotanic acid, Digallic acid, Tannimum, Quercotannic acid
Physical state	Solid
Molecular formula	$C_{76}H_{52}O_{46}$
Molecular weight	1701.2 g/mole
Color	Reddish brown.
Melting point	Decomposes above 200 °C
Solubility:	2850 g/L. Highly soluble in water

1.3 VARIOUS METHODS FOR REMOVAL OF TANNIC ACID

Various physico-chemical and biological methods are used to remove dissolved organic matter from wastewaters. In physico-chemical methods, coagulation, adsorption, electro-chemical treatment, membrane separation and biological methods are used (Lin et al., 2008 ; He et al., 2006 ; Cheng et al., 2005 ; Mark et al., 2007). It is well known that the traditional coagulation process is not effective in removing low molecular disinfection by-products. Though membrane separation process provides very high removal efficiency of dissolved organic matter in drinking water treatment, however, it has limited tannic acid removal capacity in practice because tannic acid tends to foul membrane severely.

Biological methods can remove 30–50% dissolved organic matter and avoid using chemicals (Figaro et al., 2007). But biological methods require complex treatment plant design and operating conditions, and are very expensive

in controlling required parameters. Among these technologies, adsorption is the most common approach for removing pollutants from water/wastewater with high efficiency and simple operating conditions (Reznik et al., 2008).

1.4 ACTIVATED CARBON AS AN ADSORBENT

Among the various treatment processes, adsorption on to activated carbon is one of the most important methods for removal of dissolved organic matter. Fig. 1.1 shows the activated carbon. Adsorption capacity of the activated carbon depends on characteristics of activated carbon's like surface area, pore size distributions, surface chemistry (surface functional groups), and ash content. Adsorption capacity also depends on adsorbate characteristics like molecular weight, polarity, p*K*a, molecular size, and functional groups. Also the condition of solution is another factor which affects the adsorption capacity. This includes pH, adsorptive concentration and presence of other possible adsorptive contaminants.

Fig. 1.1: Activated Carbon

Activated carbon has an extremely large surface area and pore volume size that gives it a unique adsorption capacity. Commercial grade activated carbon products surface area range between 300 and 2,000 m^2/g (Burdock, 1997). Some have very high surface areas as 5000 m^2/g.

Table 1.2 shows the adsorption capacities of various adsorbents. We can see that the adsorption capacity of commercial activated carbon is highest at 980.3 mg/g. Activated carbon can be recycled and reactivated, or regenerated from spent activated carbon.

The primary use for activated carbon is the treatment of water, including potable water (24% of all use); wastewater (21%) and groundwater remediation (4%) (Baker et al., 1992). Activated charcoal is also used to filter tobacco smoke. There are also a number of applications related to purification in the clothing, textile, personal care, cosmetics, and pharmaceutical industry.

Activated carbon is also used as decolorizing agent; as taste- and as odor-removing agent; as purification agent in food processing (Food Chemicals Codex, 1996). Food and beverage production accounts for only about 6% of the market for liquid-phase activated carbon (Baker, et al., 1992). Of this, the greatest use is decolouring sugar. More recent applications have enabled the production of xylose and its derivatives from complex cellulose sources via fermentation and activated charcoal (Mussatto and Roberto, 2001).

Table 1.2. Adsorption capacities of various adsorbents.

Adsorbent	Adsorption capacity (mg/g)
Commercial activated carbon	980.3
Activated carbon produced from New Zealand coal	588
Filtrasorb 400	476
Activated carbon	400
Activated carbon produced from Venezuelan bituminous coal	380
Peat	324
Coal	323.68
Filtrasorb 400	299
Norit	276
Picacarb	246
Filtrasorb 300	240
Activated carbon	238
Coal	230
Commercial activated carbon	200
Bituminous coal	176
Charcoal	62.7
Activated carbon	9.81
BFA	6.46
Red mud	2.49
Spent tea leaves	300.5
Zeolite	10.82
Papaya seeds	555.55
Pineapple stem	119.05

Source: Rafatullaha et al., 2001.

1.5 OBJECTIVES

The following aims and objectives have been set for the present work.

1. To study the effect of initial pH, adsorbent dose, contact time, initial concentration, and temperature on the removal of TA from the aqueous solution in batch study.
2. To perform the equilibrium adsorption and the kinetics of adsorption of TA onto ACC and to analyze the experimental data using various kinetic and isotherm models.
3. To perform desorption study for the possible regeneration of adsorbent.

CHAPTER- 2

ADSORPTION THEORY

2.1 GENERAL

Adsorbent surfaces contain unsaturated bonds and this bond is responsible for the reactant molecules to get attached to the surface. The degree of interaction depends on the nature of adsorbate and the adsorbent. Depending on the nature of interaction, adsorption is classified as either physical or chemical also called as physisorption and chemisorption adsorption respectively. Physisorption is caused by the forces of molecular interaction, which include dipole and dispersive forces and thus, physisorption is a result of the same forces that cause condensation and solidification of fluid phases. On the contrary, chemisorption involves interaction of electrons of the adsorbate and adsorbent resulting in the formation of a chemical bond. Unfortunately, it is not always easy to determine experimentally predict whether physi- or chemi-sorption is taking place. Table 2.1 gives a comparison between physical and chemical adsorption. If the heat of adsorption is very large or if the adsorption has higher activation energy than the latent heat of evaporation, then the adsorption is clearly chemisorption. Unfortunately, often the heat of adsorption is about 40-50 kJ/mol. In this case, it is very difficult to determine whether the adsorption is physical or chemical. Other criteria, which are helpful in distinguishing between these two types of adsorption, are electrical conductivity (which changes appreciably upon adsorption) and FTIR spectroscopy.

2.2 PROCESS OF ADSORPTION

The rate of adsorption is determined by the rate of transfer of the adsorbate from the bulk solution to the adsorption sites. The transport of components from

the solution phase into the pores of the adsorbent particles may be controlled either by one or more of the following steps: film or external diffusion, pore diffusion, surface diffusion and adsorption on the pore surface. It is necessary to calculate the slowest step involved among these steps to identify the controlling step during the adsorption process (Srivastava and Srivastava, 2009). The external mass transfer controls the adsorption process for the systems that have poor mixing, dilute concentration of adsorbate, small particle sizes of adsorbent and higher affinity of adsorbate for adsorbent. Whereas, the intraparticle diffusion controls the adsorption process for a system with good mixing, large particle sizes of adsorbent, high concentration of adsorbate and low affinity of adsorbate for adsorbent (Aravindhan et al., 2007).

As the adsorbate concentration increases, adsorption occurs in three stages. First, a single layer of molecules builds up over the surface of the solid. This monolayer may be chemisorbed and is associated with a change in free energy that is a characteristic of the forces that hold it. Second, as the fluid concentration is further increased, second, third etc., layers form by physical adsorption. The numbers of layers which can form are limited by the size of the pores. Finally, for adsorption from the gas phase, capillary condensation may occur in which capillaries become filled with condensed adsorbate, when its partial pressure reaches a critical value relative to the size of the pore.

The parameters that affect the adsorption process are initial pH (pH_i), adsorbent dose (m_{ad}), contact time (t) and temperature (T).

Table 2.1. Comparison between physisorption and chemisorption (Ruthven, 1984).

Property	Physisorption	Chemisorption
Heat of adsorption	Low (< 2-3 times latent heat of evaporation)	High (> 2-3 times latent heat of evaporation)
Rate of adsorption	Rapid, non activated, Reversible	Activated, may be slow and irreversible
Rate of desorption	Activation energy for desorption equals heat of adsorption	Activation energy for desorption may be larger than heat of adsorption
Temperature range over which adsorption occurs	Close to condensation temperature of the adsorbate	Occurs at a wide range of temperatures and at temperatures much above the condensation temperature.
Electrical conductivity	Electrical conductivity of the catalyst not affected	May affect electrical conductivity of catalyst

2.3 ADSORPTION KINETICS

Pseudo-first-order model: The adsorption of adsorbate from solution to adsorbent can be considered as a reversible process with equilibrium being established between the solution and the adsorbate. Assuming a non-dissociating molecular adsorption of adsorbate molecules on adsorbent, the sorption phenomenon can be described as the diffusion controlled process.

Using first order kinetics it can be shown that with no adsorbate initially present on the adsorbent, the uptake of the adsorbate by the adsorbent at any instant t is given as (Srivastava et al., 2006):

$$q_t = q_e [\, 1 - exp\,(- k_f t\,)] \qquad (2.1)$$

where, q_e is the amount of the adsorbate adsorbed on the adsorbent under equilibrium condition, k_f is the pseudo-first order rate constant, t is the time, q_t is the amount of the adsorbate adsorbed on the adsorbent in time t.

Pseudo-second-order model: This is represented as (Ho and McKay, 1999):

$$q_t = \frac{tk_S q_e^2}{1 + tk_S q_e} \qquad (2.2)$$

The initial sorption rate, h (mg/g min), at t –> 0 is defined as

$$h = k_S q_e^2$$

2.4 INTRA-PARTICLE DIFFUSION STUDY

The possibility of intra-particle diffusion can be explored by using the intra-particle diffusion model.

$$q_t = k_{id} t^{1/2} + I \qquad (2.3)$$

where, k_{id} is the intra-particle diffusion rate constant, and values of I give an idea about the thickness of the boundary layer.

In order to check whether surface diffusion controls the adsorption process, the kinetic data were further analyzed using Boyd kinetic expression which is given by (Boyd et al., 1947):

$$F = 1 - \frac{6}{\pi^2} \exp(-B_t) \text{ or } B_t = -0.4977 - \ln(1 - F) \qquad (2.4)$$

Where, $F(t) = q_t/q_e$ is the fractional attainment of equilibrium at time t, and B_t is a mathematical function of F.

However, if the data exhibit multi-linear plots, then two or more steps influence the overall adsorption process. In general, external mass transfer is characterized by the initial solute uptake and can be calculated from the slope of plot between C/C_o versus time. The slope of these plots can be calculated either by assuming polynomial relation between C/C_o and time or it can be calculated based on the assumption that the relationship was linear for the first initial rapid phase.

2.5 ADSORPTION ISOTHERM

Equilibrium adsorption equations are required in the design of an adsorption system and their subsequent optimization (Sharma et al., 2010). Therefore it is important to establish the most appropriate correlation for the equilibrium isotherm curves. Srivastava et al., (2007) have discussed the theory associated with the most commonly used isotherm models. Various isotherms namely Freundlich, Langmuir, Redlich-Peterson (R-P) and are widely used (Table 2.2).

The Freundlich isotherm is derived by assuming a heterogeneous surface with a non-uniform distribution of heat of adsorption over the surface, whereas in the Langmuir theory the basic assumption is that the sorption takes place at specific homogeneous sites within the adsorbent. The R-P isotherm incorporates three parameters and can be applied either in homogenous or heterogeneous systems.

Table 2.2. Various isotherm equations for the adsorption process

Isotherm	Equation	Reference
Freundlich	$q_e = K_F C_e^{1/n}$	(Freundlich, 1906)
Langmuir	$q_e = \frac{q_m K_L C_e}{1 + K_L C_e}$	(Langmuir, 1918)
R-P	$q_e = \frac{K_R C_e}{1 + a_R C_e^{\beta}}$	(Redlich and Peterson, 1959)

K_R: R–P isotherm constant (l/g), a_R: R–P isotherm constant (l/mg), β: Exponent which lies between 0 and 1, C_e: Equilibrium liquid phase concentration (mg/l), K_F: Freundlich constant (l/mg), 1/n: Heterogeneity factor, K_L: Langmuir adsorption constant (l/mg), q_m: adsorption capacity (mg/g).

CHAPTER- 3

LITERATURE REVIEW

In this chapter, various adsorption studies of TA on varieties of adsorbent, available in open literature, have been reviewed (Table 3.1).

Lin et al., (2011) studied surfactant-modified zeolites (SMZs) with various loadings of cetylpyridinium bromide (CPB) as adsorbents to remove tannic acid from aqueous solution. The tannic acid adsorption efficiencies for natural zeolite and various SMZs were compared. SMZ presented higher tannic acid adsorption efficiency than natural zeolite, and SMZ with higher loading amount of CPB exhibited higher tannic acid adsorption efficiency. The adsorption of tannic acid onto SMZ as a function of contact time, initial adsorbate concentration, temperature, ionic strength, coexisting Cu(II) and solution pH was investigated. The adsorption kinetics of tannic acid onto SMZ with CPB bilayer coverage (SMZ-CBC) followed a pseudo-second order model. The equilibrium adsorption data of tannic acid onto SMZ-CBC were well represented by Langmuir and Redlich-Peterson isotherms. The calculated thermodynamic parameters indicated that tannic acid adsorption onto SMZ-CBC was spontaneous and exothermic. The tannic acid adsorption capacity for SMZ-CBC slightly decreased with increasing ionic strength but significantly increased with increasing Cu(II) concentration. The tannic acid adsorption capacity for SMZ-CBC was relatively high at solution pH 4.0–7.0, and decreased with an increase in solution pH from 7.0 to 8.5. The mechanisms controlling tannic acid adsorption onto SMZ-CBC at solution pH 5.5 included electrostatic attraction, hydrogen bonding and organic partitioning.

Wang et al., (2011) studied the behavior and mechanism of tannic acid adsorption on an amino-functionalized magnetic nanoadsorbent. Amino-functionalized magnetic nanoadsorbent (Fe_3O_4@SiO_2-NH_2) exhibited high adsorption capacity for aqueous tannic acid with maximum adsorption amount of 136.23 mg/g at 25 °C. Tannic acid adsorption on the adsorbent could be well described by Langmuir adsorption model and the adsorption process was endothermic. Furthermore, pseudo-second adsorption kinetics fitted tannic acid adsorption data very well, and the adsorption rate decreased with increasing initial tannic acid concentration. The presence of Na^+, K^+, and Ca^{2+} may result in enhanced tannic acid adsorption. In addition, tannic acid adsorption over the adsorbent was highly dependent on solution pH and the maximum adsorption amount was found to be at pH 6.0. The X-ray photoelectron spectroscopy (XPS) analysis revealed that tannic acid adsorption over the adsorbent may be attributed to the surface complexation between the amino groups of the adsorbent and tannic acid in solution. It was seen that the tannic acid loaded adsorbent can be effectively desorbed in a 0.5 M HCl solution, and the regenerated adsorbent can be recycled.

Wang et al., (2010) studied the tannic acid adsorption on amino-functionalized magnetic mesoporous silica. Amino functionalized magnetic mesoporous silica (magMCM-41-NH_2) was prepared and adsorption of organic pollutant tannic acid from aqueous solution on the resulting material was investigated. Batch adsorption tests indicated that magMCM-41-NH_2 adsorbent exhibited high adsorption affinity towards aqueous tannic acid with a maximum adsorption capacity of 510.2 mg/g. The Freundlich model could fit the adsorption isotherm of tannic acid over magMCM-41-NH_2 very well, implying that adsorption process was heterogeneous. Tannic acid adsorption on magMCM-41-

NH_2 could be well described by the pseudo-second-order kinetics. Adsorption of tannic acid on the adsorbent was found to be strongly dependent on pH and ionic strength, suggesting that electrostatic interaction played a crucial role in tannic acid adsorption. X-ray photoelectron spectroscopy (XPS) analysis confirmed the formation of complex compound between tannic acid and surface amino groups of magMCM-41-NH_2 upon adsorption.

Wang et al., (2010) studied the adsorption and desorption of tannic acid on commercial resins XAD-7 and D-201 and all data indicated that resin XAD-7 could be used as an effective adsorbent for removing tannic acid during water/wastewater treatment. Furthermore, adsorption thermodynamics studies indicated different adsorption mechanisms for tannic acid on XAD-7 and D-201. FT-IR and solid state 13C-NMR spectroscopy were used to explain the adsorption force between XAD-7 and tannic acid. 13C-NMR and FT-IR spectroscopy characterization of XAD-7 indicated that the hydrogen bonding between resin's C = O and tannic acid HO— groups was the main adsorption force. Tannic acid adsorbed by XAD-7 could be desorbed using NaOH solutions completely. So XAD-7 may be used as an effective adsorbent to remove tannic acid from water/wastewater. The values of the enthalpy for tannic acid adsorbed by XAD-7 were negative, indicating an exothermic reaction, and their magnitudes (< 43 kJ·mol−1) showed the process to be a physical adsorption. But the values of the enthalpy for tannic acid adsorbed by D-201 are positive, which indicated an endothermic reaction, and their magnitudes (> 43 kJ·mol−1) manifested the process to be a chemical adsorption. XAD-7's adsorption capacity for tannic acid was measured in the presence of metal ions. Though Mg^{2+} and

Ca^{2+} , affected XAD-7's adsorption capacity for tannic acid slightly, Cu^{2+} and Pb^{2+} decreased XAD-7's adsorption capacity significantly.

Wang et al., (2009) studied the adsorption of tannic and gallic acids on a new polymeric adsorbent and the effect of Cu(II) on their removal. A new polymeric adsorbent WJN-09 for adsorbing and removing tannic and gallic acids from water was prepared, and its adsorption capacities for these two natural organic acids were tested by using the commercial resins XAD-7, XAD-4 and NDA-7 as references. The adsorption capacities of WJN-09 for tannic and gallic acids were higher than those of XAD-4, XAD-7 and NDA-7 at 303 K, which may be attributed to its amino function groups, pore structure and Zeta potential. The adsorption enthalpy changes (>43 kJ mol−1) exhibited that the adsorption of tannic acid by WJN-09 was a chemical and endothermic process. Furthermore, batch kinetic studies indicated that the tannic acid adsorbed to WJN-09 could be fitted well by both pseudo-first-order and pseudo-second-order adsorption equations, but the intraparticle diffusion played a dominant role in the adsorption of gallic acid. Changes of resin's Zeta potential and acids' average molecular size were observed when Cu(II) was added in solutions, which could explain the significant increase in WJN-09's adsorption capacity for tannic and gallic acids in the presence of Cu(II).

An and Dultz (2007) studied the adsorption of tannic acid on chitosan-montmorillonite as a function of pH and surface charge properties. Chitosan, a natural biopolymeric cation, is a candidate to modify montmorillonite for the adsorption of anions. As an anionic organic pollutant the adsorption of tannic acid was studied. Because of protonation/deprotonation reactions of both chitosan-montmorillonite and tannic acid, the adsorption process is strongly pH-dependent. The objective here was to characterize the pH dependency of

adsorption in combination with surface charge determinations. Montmorillonite was modified with different amounts of chitosan, corresponding to 20–1000% of the cation exchange capacity (CEC). The adsorption capacity for tannic acid was investigated with the batch technique at pH 3, 4, 5 and 8. As a measure for the adsorption properties, the electrokinetic surface charge was determined with a particle charge detector. The uptake of chitosan by montmorillonite was up to 152% (1.69 molc kg−1) of the CEC. The resulting anion exchange capacity of chitosan-montmorillonite calculated from C-content was 0.43 molc kg−1. At low loadings with chitosan (24.7 and 49.5% uptake), a monolayer was formed in montmorillonite. At an uptake of 96.8%, a bilayer structure was observed, which becomes more dominant at higher loadings. On the external surface, a monolayer of chitosan was formed. The maximal adsorption capacity for tannic acid was found with 240 g kg−1 (0.14 molc kg−1) at pH 4. The adsorption process fitted in well with the Freundlich isotherm. At lower as well as higher pH values the adsorption capacity decreased up to about 25%. Most probably the exchange sites in the interlayer did not contribute to the adsorption of tannic acid. The observed surface charge was lower than the adsorbed amount of tannin. It was thought that tannin was adsorbed also by van der Waals forces besides ionic forces.

Ucer et al., (2006) investigated the adsorption of the toxic metal ions onto tannic acid immobilised activated carbon depending on pH, contact time, carbon dosage, adsorption capacity and adsorption isotherms by employing batch adsorption technique. In the optimum conditions, the percent adsorption of metal ions were determined for Cu(II) (23.5%), Cd(II) (17.8%), Zn(II) (14.0%), Mn(II) (11.3%) and Fe(III) (17.9%) and results were compared with that of the untreated activated carbon. The order of affinity based on uptake by tannic acid immobilised activated carbon and untreated activated carbon was the same as

Cu(II) > Fe(III) > Cd(II) > Zn(II) > Mn(II), but differing in the adsorption capacities. The adsorption data was correlated to Langmuir and Freundlich isotherm for each metal ion and the data fitted better to the Langmuir isotherm model. A combined ion exchange, complex formation and surface adsorption processes were believed the major adsorption mechanisms playing role in the binding of metal ions. Adsorbed metal ions were effectively desorbed (90.2–98.4%) by using 0.1M HCl without destroying the modified adsorbent.

Ucer et al., (2005) studied the immobilisation of tannic acid onto activated carbon to improve Fe(III) adsorption. commercially available tannic acid was employed in the modification of the surface properties of granulated activated carbon and optimum experimental parameters such as pH, contact time, initial concentration, adsorption capacity and adsorption isotherms for (a) tannic acid immobilisation onto activated carbon and (b) Fe(III) adsorption on tannic acid-activated carbon combination were determined at room temperature. Adsorption of Fe(III) on granulated activated carbon alone was also determined to compare the experimental results. Tannic acid was found effective to enhance the metal adsorption capacity of activated carbon surfaces. The Langmuir isotherm equation was found to provide reasonable well fit for the tannic acid-activated carbon and Fe(III)–tannic acid-activated carbon combinations. Recovery studies showed that adsorbed Fe(III) ions could be recovered (96.1±1.3%) by using 0.1M HCl without destroying the modified adsorbent.

Chang and Juang (2004) studied the adsorption of tannic acid, humic acid, and dyes from water using the composite of chitosan and activated clay. Chitosan is a well-known excellent adsorbent for a number of organics and metal ions, but its mechanical properties and specific gravity should be enhanced for practical operation. Activated clay was added in chitosan slurry to prepare composite

beads. The adsorption isotherms and kinetics of two organic acids (tannic acid, humic acid) and two dyes (methylene blue, reactive dye RR222) using composite beads, activated clay, and chitosan beads were compared. With composite beads as an adsorbent, all the isotherms were better fitted by the Freundlich equation. The adsorption capacities with composite beads were generally comparable to those with chitosan beads but much larger than those with activated clay. The pseudo-first-order and pseudo-second-order equations were then screened to describe the adsorption processes. It was shown that the adsorption of larger molecules such as tannic acid (MW, 1700 $gmol^{-1}$), humic acid, and RR222 from water onto composite beads was better described by the pseudo-first-order kinetic model. The rate parameters of the intraparticle diffusion model for adsorption onto such adsorbents were also evaluated and compared to identify the adsorption mechanisms.

Table 3.1: Various adsorption studies of Tannic Acid

Adsorbate	Adsorbent	Isotherm	Model	Results/Conclusion	Reference
Tannic Acid	Surfactant-modified zeolites with loadings of cetylpyridinium	Langmuir and Redlich-Peterson	Pseudo-second-order	Natural zeolite had little affinity for tannic acid. Surfactant-modified zeolites presented higher adsorption capability of tannic acid with higher loadings of cetylpyridinium	Lin et al., 2011
Tannic Acid	Amino functionalized magnetic nanoadsorbent	Langmuir	Pseudo-second-order	The adsorption of tannic acid on amino funtionalized magnetic nanoadsorbent exhibited high capacity. This may be attributed to the surface complexation between adsorbent and tannic acid in solution.	Wang et al., 2011
Tannic Acid	Amino functionalized magnetic mesoporous silica	Freundlich	Pseudo-second-order	High adsorption capacity was seen between tannic acid and amino functionalized mesoporous silica. Adsorption was highly pH and ionic strength dependent.	Wang et al., 2010
Tannic Acid	Commercial resins Xad-7 and D-201	Langmuir	__	XAD-7 is found to be very efficient in removing tannic acid from wastewater. Hydrogen bonding between tannic acid and resin is the main cause for adsorption.	Wang et al., 2010
Tannic Acid and Gallic Acid	Polymeric adsorbent WJN-09	Freundlich	Pseudo-first-order and pseudo-second-order	WJN-09 showed higher adsorption capacity than comercial resins XAD-7, XAD-4, owing to its amino groups, pore structure, and zeta potential.	Wang et al., 2009
Tannic Acid	Chitosan-montmorillonite	Freundlich	__	The adsorption of chitosan on montmorillonite is combined with an uptake of cation–anion pairs. Due to the adsorption of anionic tannic acid only on the external surface,the adsorption is considerably lower.	An and Dultz, 2006

Toxic metal ions	Tannic acid immobilised activated carbon	Langmuir	__	Adsorption capacity of tannic acid immobilised activated carbon for toxic metal ions uptake was higher as tannic acid immobilization improves the existing properties of activated carbon for adsorption.	Ucer et al., 2005
Tannic Acid, Humic Acid and dyes	Composite of chitosan and activated clay	Freundlich	Pseudo-first-order	The composite beads showed adsorption of tannic and other acids comparable to that of activated clay, and the adsorption was better described by pseudo-first-order model.	Chang and Juang, 2004
Fe(III)	Tannic acid immobilised activated carbon	Langmuir	__	Tannic acid immobilised on activated carbon is found to be more efficient in removing Fe(III) ions than activated carbon slone	Ucer et al., 2004

CHAPTER- 4

MATERIALS AND METHODS

4.1. Wastewater

Aqueous solution of TA was taken as wastewater. Initially 1g/l of stock solution was prepared which was diluted to make the working solution to suit the feasibility of experiments.

4.2. Adsorbent and its BET Surface Area

Coconut-based granular ACC was supplied by Pneumatic Engineers Spares & Service, New Delhi, India.

It was used as procured, except for the removal of very fine particles by sieving. Pore sizes are classified in accordance with the classification of International Union of Pure and Applied Chemistry (IUPAC) [IUPAC, 1982], that is, micro-pores (diameter (d) < 20 Å), meso-pores (20 Å < d < 500 Å) and macro-pores (d > 500 Å). Micro-pores can be divided into ultra micro-pores (d < 7 Å) and super micro-pores (7 Å < d < 20 Å). For larger sizes of liquid molecules, the adsorbents for liquid phase adsorbates should have predominantly meso-pores in the structure. The BET surface area of ACC is was found to be 222.33 m^2/g, whereas the BET average pore diameter of ACC is found to be 26.56 Å. Therefore, ACC has meso-porous nature which is desirable for adsorption of high weight molecules.

4.3. Analytical Methods

The determination of the concentration of TA was performed by finding out the absorbance characteristic wavelength using UV/VIS spectrophotometer (Perkin Elmer, Schimadzu, Japan). A solution of known concentration was taken and the absorbance was determined at different wavelengths to obtain a plot of absorbance versus wavelength. The wavelength corresponding to maximum absorbance (λ_{max}) was determined. The λ_{max}

for TA were found to be 283 nm. Calibration curve was plotted between the absorbance and the concentration of TA solution (Fig.4.1).

4.4. Experimental Programme

For each experiment, a known amount of the adsorbent was introduced into 250 ml stoppered conical flasks in which 100 ml of the TA slution of known pH_i was already present. This was kept in a temperature-controlled shaker at a constant speed of 120 rpm at a pre-decided constant temperature for 7h to attain the equilibrium. The adsorbent and adsorbate was separated from the TA solution after 7 h and analysed for concentration. The percentage removal of TA was calculated using the following relationship:

$$\text{Percent TA removal} = \frac{(C_0 - C_e)100}{C_0} \qquad (4.1)$$

Where, C_o is initial TA concentration and C_e is the equilibrium TA concentration (mg/l).

The adsorption of TA by ACC was studied over a initial pH (pH_i) range of 3–10 at 301 K. The pH_i of the adsorbate solutions was adjusted using 1 N aqueous solution of either H_2SO_4 or NaOH. The adsorbent dosage (m_{ad}) value was kept constant at 20 g/l during pH study. Dosage study was carried out by varying the adsorbent dosages (m_{ad}) in the range of 0.5-2.5 g/l for ACC at the optimum pH_i ($pH_{i\text{-}opt}$) and 301 K.

4.4.1. Kinetics of adsorption: Kinetic parameters were calculated using pseudo-first-order and pseudo-second-order model at various C_0 values (50-200 mg/l) at optimum m_{ad} ($m_{ad\text{-}opt}$) of ACC. The amount of adsorbate adsorbed, q_t (mg/g), at any time t was calculated as:

$$q_t = \frac{(C_0 - C_t)}{m_{ad}} V \qquad (4.2)$$

Where, C_t is the TA concentration (mg/l) at time t, V is the volume of the solution (litre).

An error function, Marquardt's percent standard deviation (MPSD) (Marquardt, 1963) was used to find out the most suitable kinetic model to represent the experimental data. This error functions is given as:

$$MPSD = 100\sqrt{\frac{1}{n_m - n_p}\sum_{i=1}^{n}\left(\frac{q_{t,i,\exp} - q_{t,i,cal}}{q_{t,i,\exp}}\right)^2} \tag{4.3}$$

In this equation, the subscript 'exp' and 'cal' represent the experimental and calculated values, n_m is the number of measurements, and n_p is the number of parameters in the model.

4.4.2. Isothermal study: Equilibrium adsorption equations are required in the design of adsorption systems. Therefore, important to establish the most suitable correlation for the equilibrium isotherm. Isothermal experiments were performed at 291, 301 and 311 K with C_0 values of 50, 100 and200 mg/l at $pH_{i\text{-}opt}$ and $m_{\boldsymbol{ad\text{-}opt}}$ of ACC. Various isotherms such as Freundlich, Langmuir and Redlich-Peterson (R-P) were used to represent the adsorption equilibrium data.

The adsorbent first separated from the TA after 7 h and analysed for equilibrium TA concentration (C_e). The equilibrium adsorption uptake, q_e (mg/g), were calculated using the following relationship:

$$q_e = \frac{(C_0 - C_e)}{w}V \tag{4.4}$$

The Chi-square error analysis function was used to find out best fit isotherm model. It is given as:

$$CHI^2 = \sum_{i=1}^{n}\frac{(q_{e,i,\exp} - q_{e,i,cal})^2}{q_{e,i,\exp}} \tag{4.5}$$

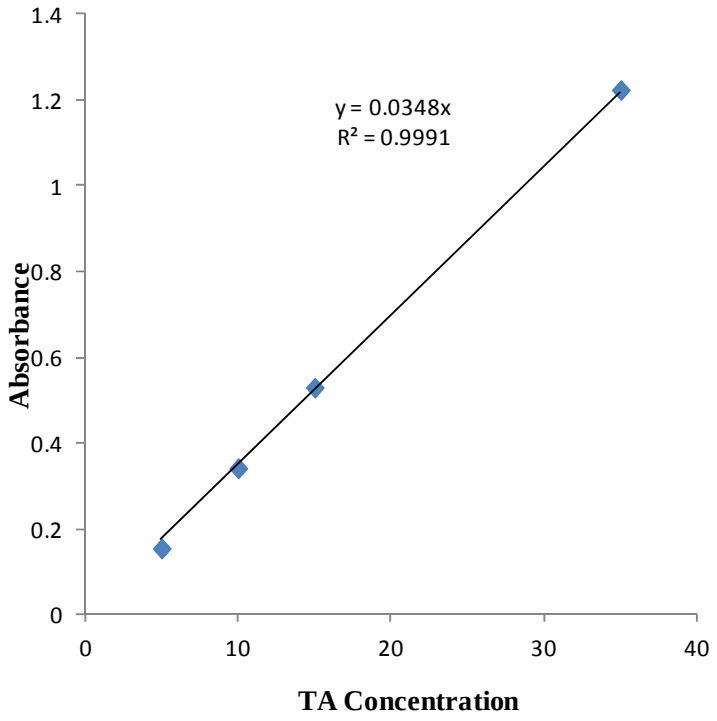

Fig. 4.1. Calibration curve for TA

4.5. Desorption

For the batch desorption study, two different studies were performed. One was a solvent desorption study and the other a thermal desorption study. In the solvent desorption study, the ACC utilized for the adsorption was separated from the solution. TA loaded ACC was then shaked at 120 rpm in a series of 250 mL conical flasks containing 50 mL of aqueous solutions (0.1 N) of C_2H_5OH, acetone and NaOH at 301 K for 24 h in the orbital shaker (Suresh et al., 2011).

In the thermal desorption study, the ACC used for adsorption of TA was separated from the solution and it was dried in an oven at 378 K for 2 h. Thereafter, dried ACC was placed in a furnace at 623 K for 4 h. The samples were taken from the furnace and kept in the desiccator. After this, the ACC was again used as adsorbent for removal of TA at 100 mg/l and 301 K. This adsorption-desorption procedure was repeated five times.

CHAPTER- 5

RESULTS AND DISCUSSION

5.1. GENERAL

This chapter reports Adsorptive treatment of Tannic Acid (TA) in batches with ACC. Results obtained during the treatment of TA and their interpretations have been discussed in detail.

5.2 Effect of Initial pH (pH_i)

Fig. 5.1 shows the effect of pH_i on the TA removal from aqueous solution by GAC at T = 301 K, t = 7 h, C_o = 100 mg/l, adsorbent dosage (m_{ad}) = 20 g/l. Highest TA removal efficiency of 67.5% and 66.02% were obtained at pH_i = 2 and 3, respectively. For all $3 < pH_i \leq 5$, very sharp decrease in TA removal efficiency was found. But, for all $pH_i > 5$, TA removal efficiency varied from 35.63- 27.54%.

TA molecules present in its molecular form at solution $pH \leq 4.5$. TA molecules are dissociated for $pH > 4.5$ and completely ionized at pH=7 (An et al., 2007). Therefore, there is higher removal efficiency for unionized TA at $pH_i \leq 3$ (Lin et al., 2011). At higher pH values the dissociation degree of TA increases leading decrease in TA removal efficiency on GAC. It also seems that, at higher pH higher OH^- ions concentration present in the solution, compete with TA adsorption onto the GAC, which reduces the TA adsorption. There is no significant differences in the TA removal at pH_i = 2 and 3, therefore, pH_i = 3 was chosen as optimum pH_i ($pH_{i\text{-}opt}$) to save the acid used for pH adjustment.

For the experiments with C_o = 100 mg/l, the final pH values (pH_f) of the adsorption process are shown as a function of pH_i in Fig. 5.1. The pH_f values are always greater than the pH_i in full studied range except for pH_i values 7 and 10.

5.3 Effect of Adsorbent Dosage (m_{ad})

The significance of m_{ad} on the adsorption of TA by ACC was studied at C_o = 100 mg/l (Fig. 5.2). An increase in ACC dosage resulted in an increase in TA removal up to a certain value and thereafter the removal efficiency remained almost constant. An increase in the removal with the increase in m_{ad} can be attributed to greater surface area and the availability of more adsorption sites. Very minute increase in TA removal was found for $m_{ad} \geq 15$ g/l f. Very minute increase in TA removal with increasing m_{ad} is due to the fact that for $m_{ad} \geq m_{ad\text{-}opt}$, the removal efficiency depends more upon the concentration of the solution and less depends upon the m_{ad}. Thus, the $m_{ad\text{-}opt}$ for TA removal from aqueous solution by ACC was 15 g/l.

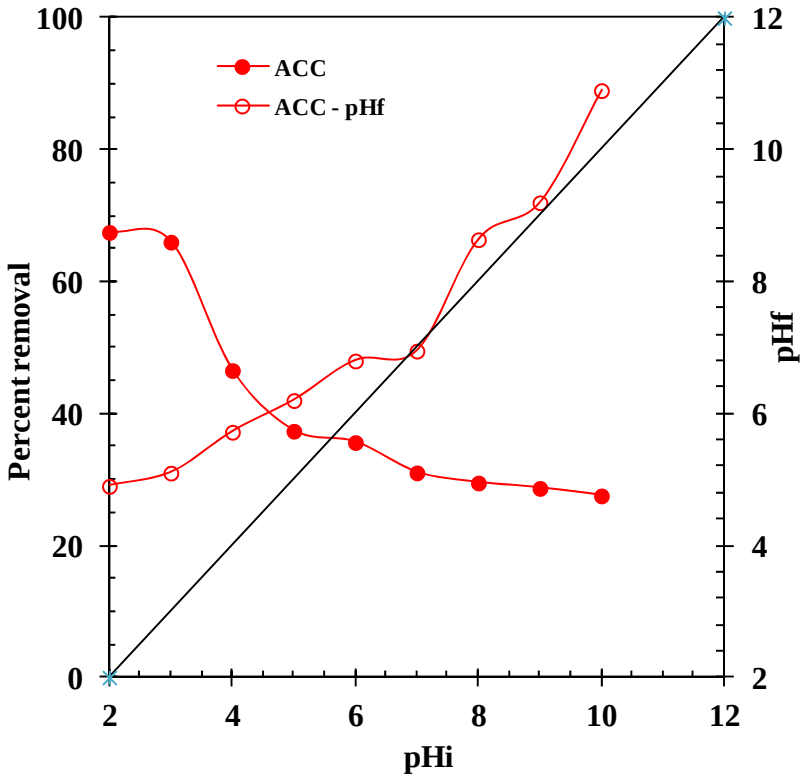

Fig. 5.1. Effect of pH_i on the TA removal by ACC (T = 301 K, t = 7 h, C_o = 100 mg/l, Adsorbent dosage (m_{ad}) = 20 g/l)

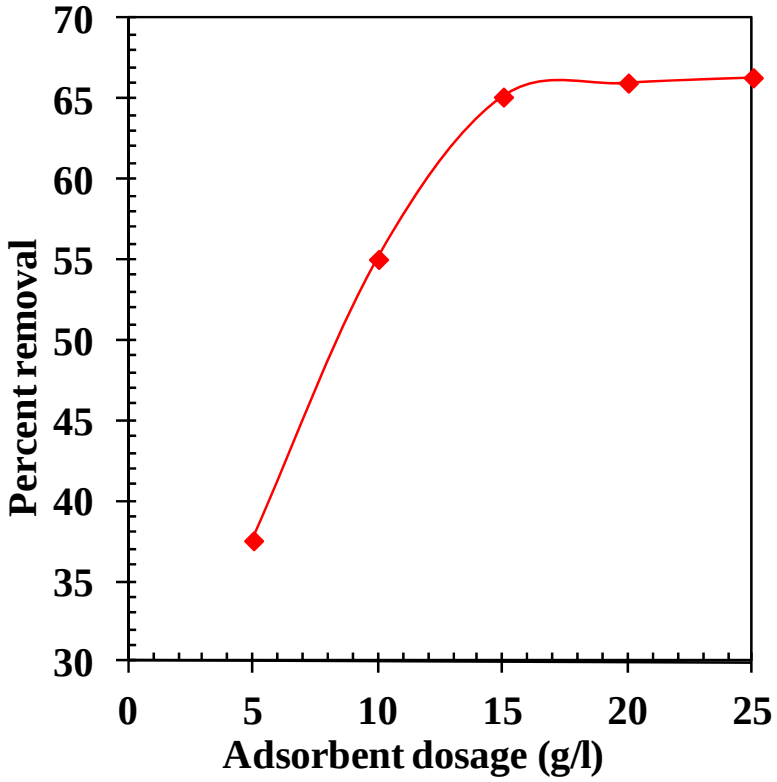

Fig. 5.2. Effect of adsorbent dosage on the TA removal by ACC (*T* = 301 K, *t* = 7 h, C_o = 100 mg/l, *pH*i = 3.0)

5.4 Effect of Time

TA aqueous solution having C_0 = 50-200 mg/l and $pH_{i\text{-}opt}$ = 3, were kept in contact with the ACC ($m_{ad\text{-}opt}$ = 15 g/l) for 7 h. Fig. 5.3 shows the effect of contact time (by data points) on adsorptive TA removal by ACC. It can be seen that TA adsorption is very rapid during first 15 min of adsorption. After 5 h, TA adsorption on ACC nearly reached the equilibrium value. This speedy adsorption of TA and reaching at equilibrium in a short period indicates the efficacy of the ACC used for its use in TA adsorption. After 5 h, no significant TA removal was observed. This may be due to the lesser availability of vacant surfaces on the solid surface and due to the lesser driving force between bulk solution and TA already adsorbed in the initial stages of adsorption. 5 h contact time can be assumed to be equilibrium time for the adsorption of TA onto ACC.

5.5 Adsorption Kinetics

Pseudo-first-order and pseudo-second-order kinetic models used to examine their validity with the experimental kinetic adsorption data. The best-fit values of the model parameters, correlation coefficients and MPSD values are given in Table 5.1. It may be concluded that pseudo second-order kinetic model with non-linear regression best fits the adsorption kinetics. The fitting of pseudo second-order model with kinetic experimental data is shown in Fig. 5.3 by solid line for TA removal by ACC.

From Table 5.1, it is observed that the q_e values increase with an increase in C_0, whereas, k_s decreases with an increase in C_0. The uptake rate is limited by the C_0 of TA and the TA affinity to the adsorbent, diffusion coefficient of the TA in the bulk and solid phases, the pore size distribution of the adsorbent, and the degree of mixing (Zogorski et al., 1976). They provide the necessary driving force to overcome the resistances to the mass transfer of TA from the aqueous solution to the

solid phases. The increase in C_0 of TA also enhances the interaction between TA and the adsorbent. The rate of adsorption also increases with the increase in C_0 due to increase in the driving force.

5.6 Controlling Mechanism

The TA transport from the solution phase into the pores of the ACC particles may be controlled either by one or more of the following steps: film or external diffusion, pore diffusion, surface diffusion and adsorption on the pore surface. It is necessary to calculate the slowest step involved among these steps to identify the controlling step during the adsorption process (Srivastav and Srivastava, 2009). It is expected that the intraparticle diffusion may be the rate controlling-step during TA adsorption onto ACC. This is due to that intraparticle diffusion controls the adsorption process for systems with good mixing, large particle sizes of adsorbent and high concentration of adsorbate (Aravindhan et al., 2007). If the Weber-Morris plot of q_t versus $t^{0.5}$satisfies the linear relationship with the experimental data, then the adsorption process is assumed to be controlled by intra-particle diffusion only. However, if the data exhibit multi-linear plots, then two or more steps influence the overall adsorption process. External mass transfer is characterized by the initial solute uptake. In the present study, it was assumed that the external mass transfer occurred in the first 15 min and that the relationship between C/C_o versus time for first 15 min was linear. The initial adsorption rates (K_s) (min^{-1}) were quantified as ($C_{15\ min}/C_o$)/15. The calculated K_s values for an initial concentration of 200,100, 50 mg/l were found to be 0.0526, 0.039, 0.04 min^{-1}, respectively.

Fig. 5.4 shows a representative q_t versus $t^{0.5}$ plot for adsorption onto ACC for C_o = 200, 100 and 50 mg/l at 301 K and $pH_{i\text{-}opt}$ = 3. In Fig. 5.4, the plots are not linear over the whole time range, implying that the more than one process is controlling the adsorption process. The first portion (line not drawn for the clarity of picture) gives the diffusion of TA through the solution to the external surface of

adsorbent. Further two linear portions depict intra-particle diffusion. The second linear portion is attributed to the gradual equilibrium stage with intra-particle diffusion dominating. The third portion is the final equilibrium stage for which the intra-particle diffusion starts to slow down due to the extremely low adsorbate concentration left in the solution. The slope of the linear portions ($k_{id,1}$ and $k_{id,2}$) defined as rate parameters and are characteristics of the rate of adsorption in the region where intra-particle diffusion is rate controlling. Extrapolation of the linear portions of the plots back to the y-axis gives the intercepts that provide the measure of the boundary layer thickness. It seems that the intra-particle diffusion of TA into mesopores (third portion) is the rate controlling step in the adsorption process. Slopes of second and third portions ($k_{id,1}$ and $k_{id,2}$) are higher for higher C_o, which corresponds to an enhanced diffusion of TA through pores. This is due to the greater driving force at higher C_o. The deviation of straight lines from the origin indicates that the pore diffusion is not the sole rate-controlling step. Therefore, the adsorption proceeds via a complex mechanism consisting of both surface adsorption and intra-particle transport within the pores of ACC.

Table 5.1. Kinetic parameters for the TA removal by ACC (t = 7 h, C_0=50-200 mg/l, m=15 g/l).

Pseudo-first-order model					
C_0 (mg/l)	$q_{e,exp}$ (mg/g)	$q_{e,calc}$ (mg/g)	k_f (min^{-1})	R^2	MPSD
200	7.341	7.344	0.013	0.96	25.54
100	4.343	3.783	0.048	0.95	24.60
50	2.547	1.967	0.043	0.78	28.20
Pseudo-second-order model					
C_o (mg/l)	$q_{e,calc}$ (mg/g)	k_s (g/mg min)	h (mg/g min)	R^2	MPSD
200	9.092	0.001	0.119	0.97	20.84
100	4.220	0.017	0.303	0.97	15.82
50	2.199	0.025	0.123	0.89	19.58

Intra-particle diffusion

C_o (mg/l)	$k_{id,1}$ (mg/g $min^{1/2}$)	I_1 (mg/g)	R^2	$k_{id,2}$ (mg/g $min^{1/2}$)	I_2 (mg/g)	R^2
200	0.386	0.99	0.96	0.126	9.92	1
100	0.109	2.27	0.989	0.032	3.66	1
50	0.0722	1.03	0.948	0.088	0.759	0.968

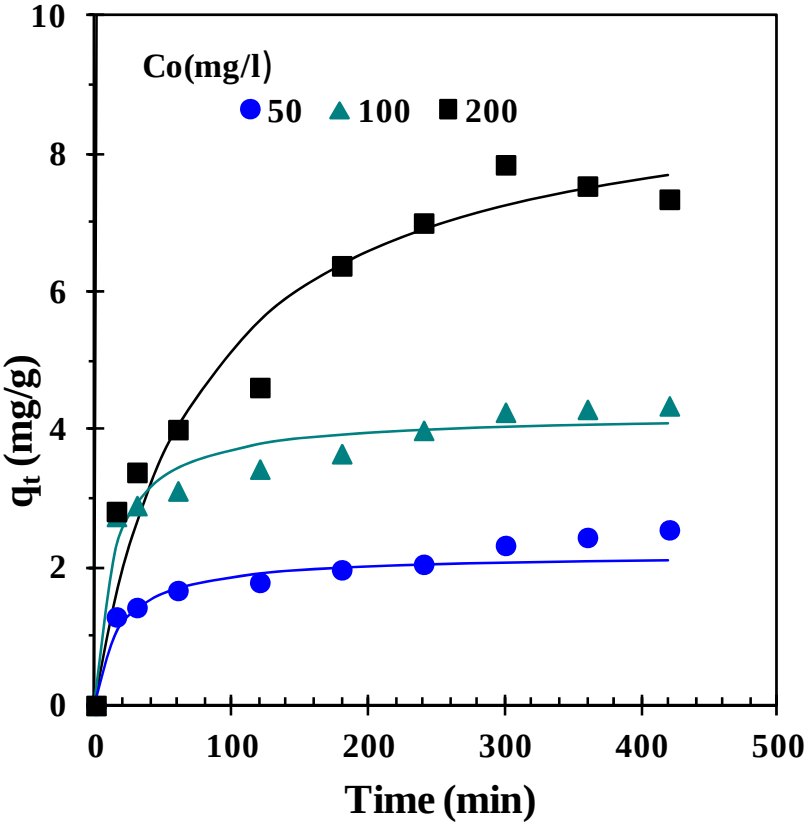

Fig. 5.3. Effect of contact time on the TA removal by ACC. Experimental data points given by the symbols and the lines predicted by the pseudo-second-order model. T = 301 K, $m_{ad\text{-}opt}$ = 15 g/l.

The multi-phasic nature of intraparticle diffusion plot confirms the presence of both surface and pore diffusion. In order to predict the actual slow step involved, the kinetic data were further analyzed using Boyd kinetic expression. Equation (2.3) was used to calculate B_t values at different time t. The linearity of the plot of B_t versus t was used to distinguish whether surface or intra-particle transport controls the adsorption rate. It was observed that the relation between B_t and t (not shown here) was non-linear (R^2 = 0.93-0.97) at all concentrations confirming that surface diffusion is the not the sole rate-limiting step. Thus, both surface and pore diffusion seem to be the rate-limiting steps in the adsorption process.

5.7 Adsorption Isotherm

5.7.1. Effect of temperature (*T*): Temperature has a significant effect on the adsorption capacity of the adsorbents. To study the effect of T on TA adsorption onto ACC was studied at different T ranging from 291-311 K. The TA adsorption onto ACC was found to increase with an increase in T. Therefore, it can be concluded that TA adsorption onto ACC is an endothermic process. Generally, adsorption is an exothermic process. However, if the adsorption process is controlled by the diffusion process (intraparticle transport-pore diffusion), the adsorption capacity will increase with an increase in temperature. This is basically due to the fact that the diffusion is an endothermic process (Srivastava et al., 2007). TA moleculer mobility increases with an increase in temperature, therefore, resistance decreases and adsorptive capacity of adsorbent increases. It is known from the previous section that the diffusion of TA into pores of the adsorbent is not the only rate-controlling step, and the diffusion process could be ignored with adequate contact time. Therefore, the increase in adsorption capacity with an increase in temperature may be attributed to chemisorptive nature of adsorption.

5.7.2. Isotherm modeling: Table 5.2 shows the values of parameters, R^2 and CHI^2 for the various isotherms (Freundlich, Langmuir and R-P isotherms) fitting to the experimental data. It may be seen in Table 5.2 that, there are marginal difference in CHI^2 and R^2 values. Any of the isotherms can be used for isotherm modeling. But generally, it may be concluded that R-P isotherm best-fits the equilibrium adsorption of TA onto ACC at all temperatures. The validation of various isotherms studied with experimental data points is shown in Fig. 5.5 by solid lines. K_F and *1/n* indicate the adsorption capacity and adsorption intensity, respectively. Higher value of *1/n* indicates the higher affinity between the adsorbate and adsorbent, and heterogeneity of the adsorbent sites. The K_F value is increasing on increasing the temperature showing higher adsorption capacity of ACC at higher temperature. This indicates the endothermic nature of adsorption of TA onto ACC. The q_m value indicates the affinity of the TA with the ACC. A high q_m value indicates a higher affinity. q_m was found to increased with increase in temperature (Table 5.2) showing higher affinity to adsorbent at higher temperature.

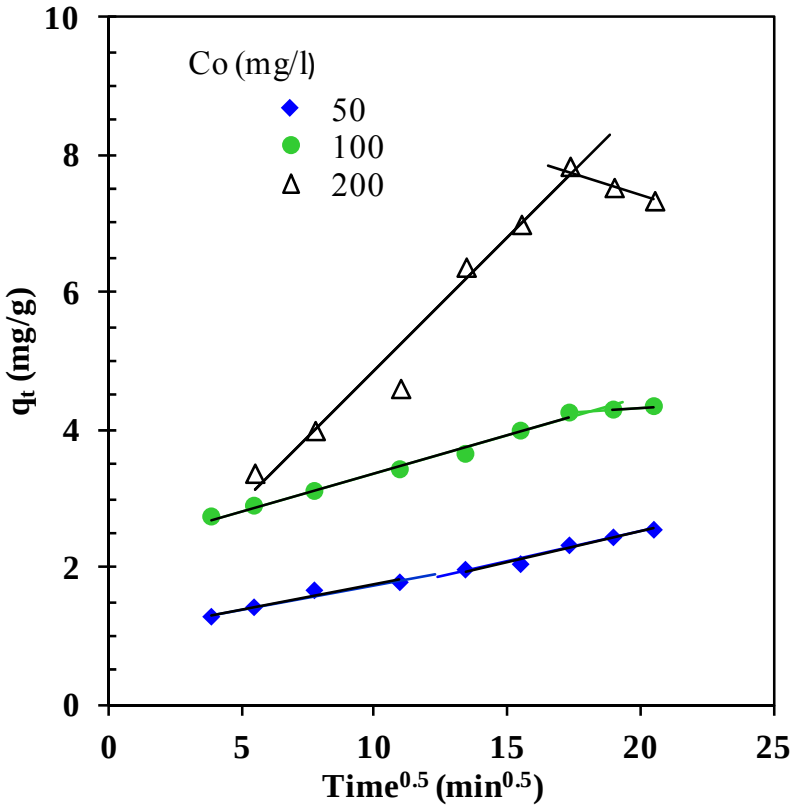

Fig. 5.4. Weber-Morris plot for the TA removal by ACC. t = 7 h, C_o = 50-200 mg/l, $m_{ad\text{-}opt}$ = 15 g/l.

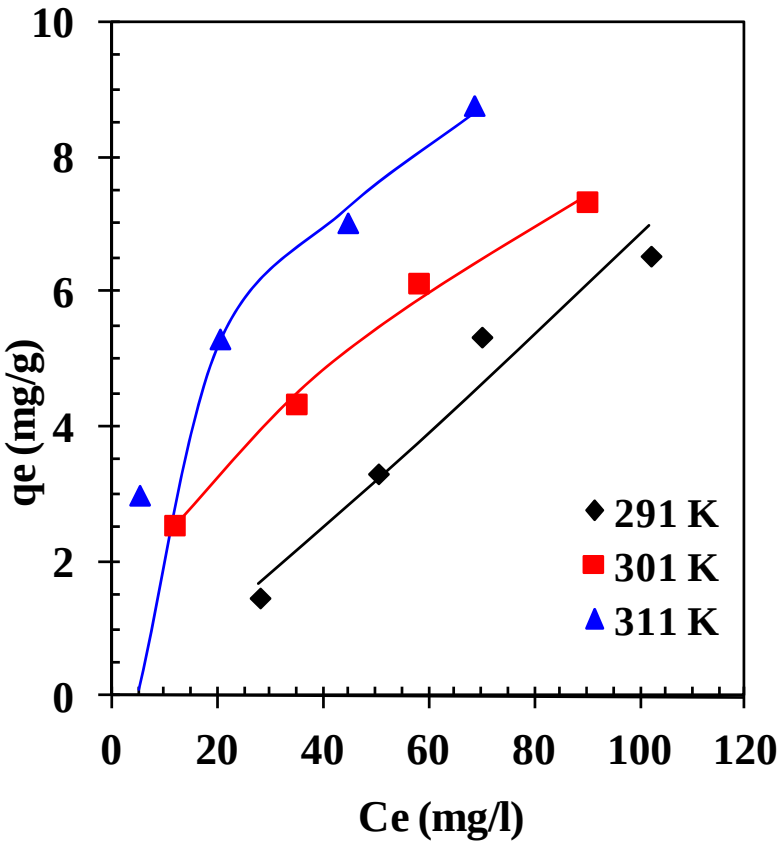

Fig. 5.5a. Equilibrium adsorption isotherms at different temperature for the TA removal by ACC. Experimental data points given by symbols and the lines predicted by Freundlich isotherm model. t = 7 h, C_o = 50-200 mg/l, $m_{ad\text{-}opt}$ = 15 g/l.

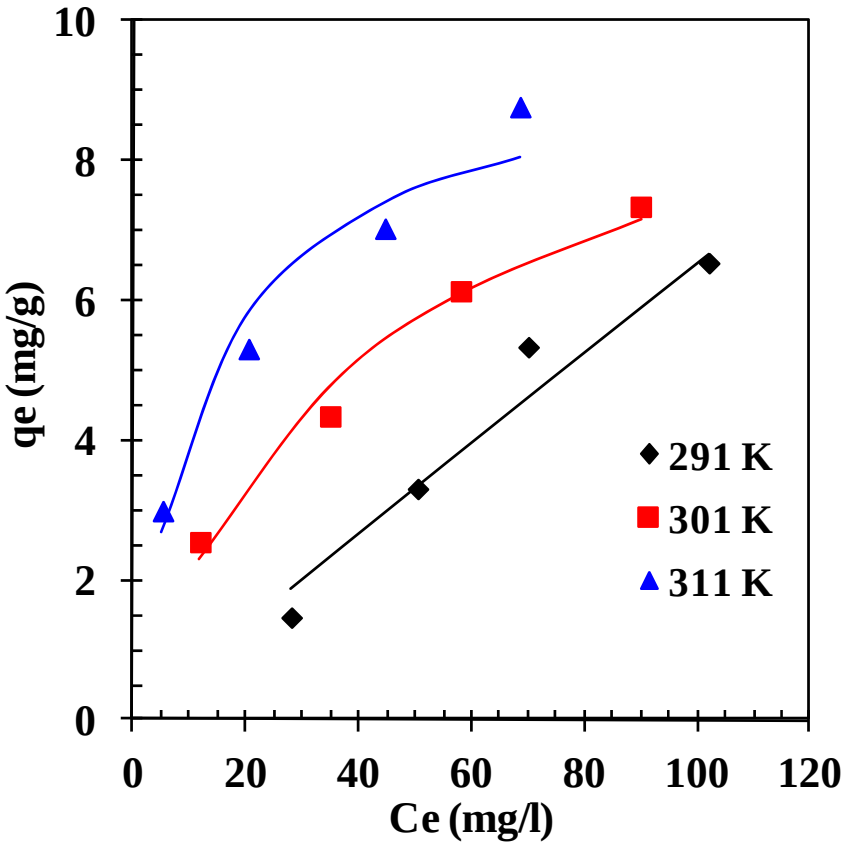

Fig. 5.5.b **Equilibrium adsorption isotherms at different temperature for the TA removal by ACC. Experimental data points given by symbols and the lines predicted by Langmuir isotherm model. t = 7 h, C_o = 50-200 mg/l, $m_{ad\text{-}opt}$ = 15 g/l.**

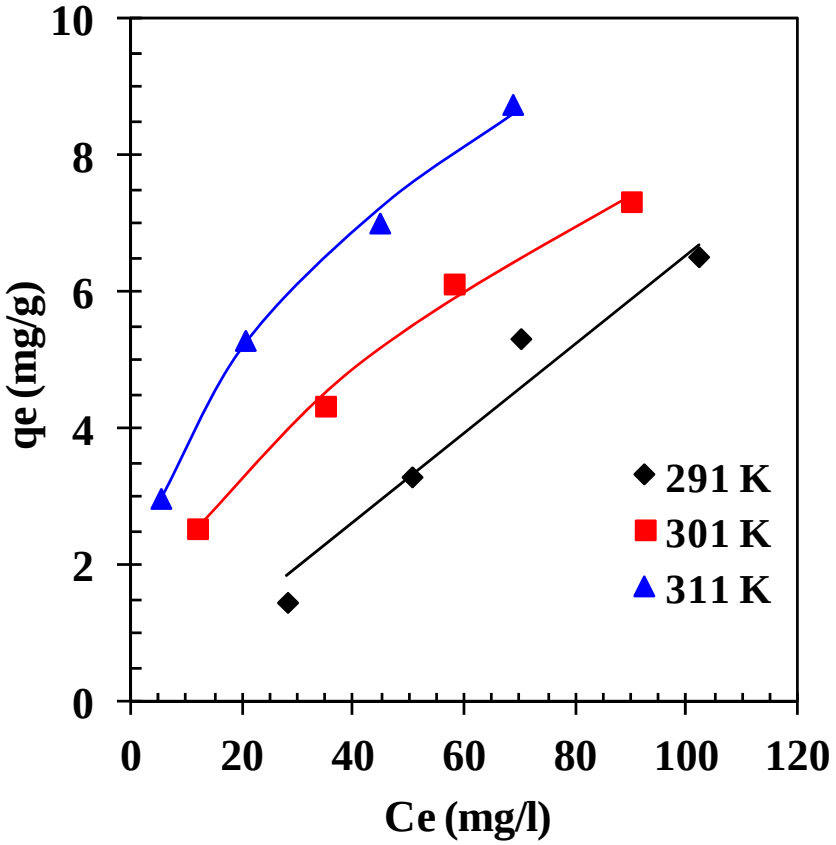

Fig. 5.5.c Equilibrium adsorption isotherms at different temperature for the TA removal by ACC. Experimental data points given by symbols and the lines predicted by R-P isotherm model. t = 7 h, C_o = 50-200 mg/l, $m_{ad\text{-}opt}$ = 15 g/l.

Table 5.2. Isotherm parameters for the TA adsorption by ACC(t = 7 h, $pH_{i\text{-}opt}$ = 3, m_{ad} = 15 g/l).

	Freundlich	$q_e = K_F C_e^{1/n}$			
T (K)	K_F ((mg/g)/(l/mg)$^{1/n}$)	*1/n*	R^2	CHI^2	
291 K	0.042	1.106	0.974	0.162	
301 K	0.679	0.532	0.997	0.016	
311 K	1.507	0.413	0.973	2.773	
	Langmuir	$q_e = \frac{q_m K_L C_e}{1 + K_L C_e}$			
T (K)	K_L (l/mg)	q_m(mg/g)	R^2	CHI^2	
291 K	0.00022	302.358	0.979	0.207	
301 K	0.02406	10.442	0.990	0.068	
311 K	0.07506	9.605	0.972	0.156	
	Redlich-Peterson	$q_e = \frac{K_R C_e}{1 + a_R C_e^{\beta}}$			
T (K)	K_R (l/g)	a_R (l/mg)$^{1/\beta}$	β	R^2	CHI^2
291 K	0.066	0.0000	0.000	0.978	0.200
301 K	2.144	2.6476	0.499	0.997	0.016
311 K	15.141	9.4584	0.600	0.998	0.009

5.8. Desorption Study

Fig. 5.6 shows the TA removal efficiency of ACC after various chemical and thermal desorption-adsorption cycles studied. Very poor desorption of TA was observed with the NaOH and ethanol and are nearly same (Fig. 5.5b,c). Acetone showed maximum desorption of TA from spent adsorbents (Fig. 5.5a).

TA desorption from spent adsorbents were also tested for the thermal desorption as described by Rathula and Srivastava (2011) and Suresh et al. (2011).

After thermal desorption of TA, unloaded ACC was again used for adsorption of TA at C_0=100 mg/l, m_{ad}=15 g/l, T=301 K and t=7 h. After adsorption of TA, loaded ACC was again exposed to thermal desorption by the same procedure. This adsorption-desorption cycle was repeated five times and results are shown in Fig. 5.5d. It can be seen that the spent ACC can be reused for several adsorption-desorption cycles.

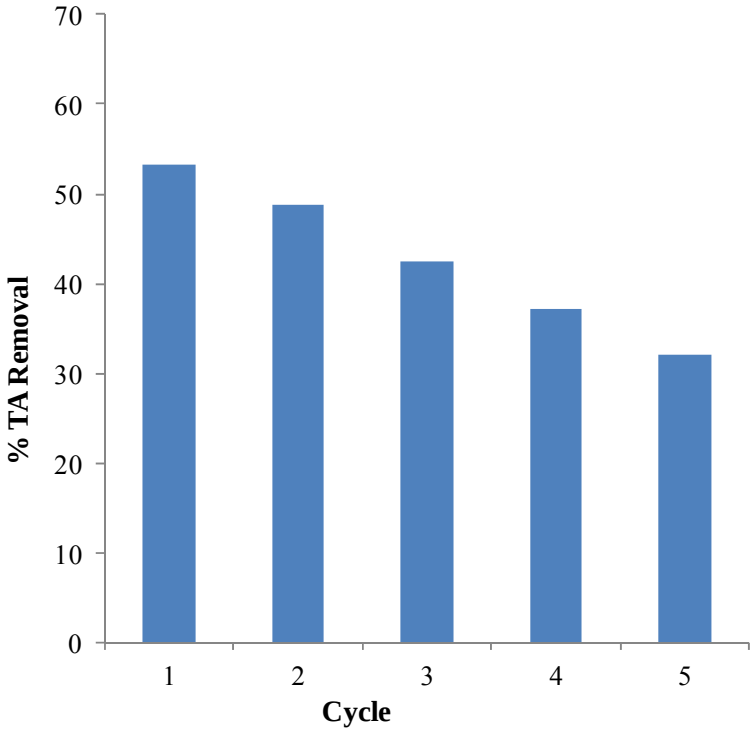

Figure 5.6a. TA removal efficiency of ACC after various desorption-adsorption cycles (with Acetone).

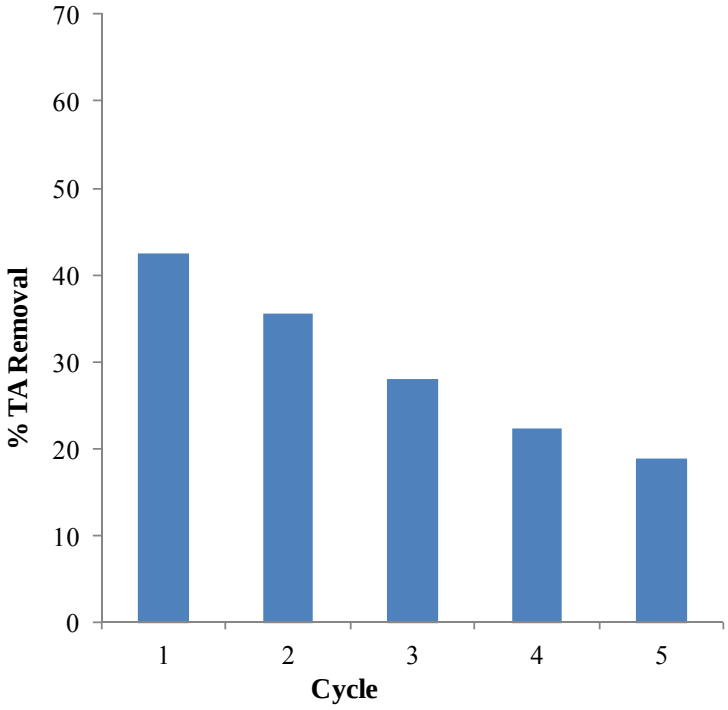

Figure 5.6b. TA removal efficiency of ACC after various desorption-adsorption cycles (with NaOH).

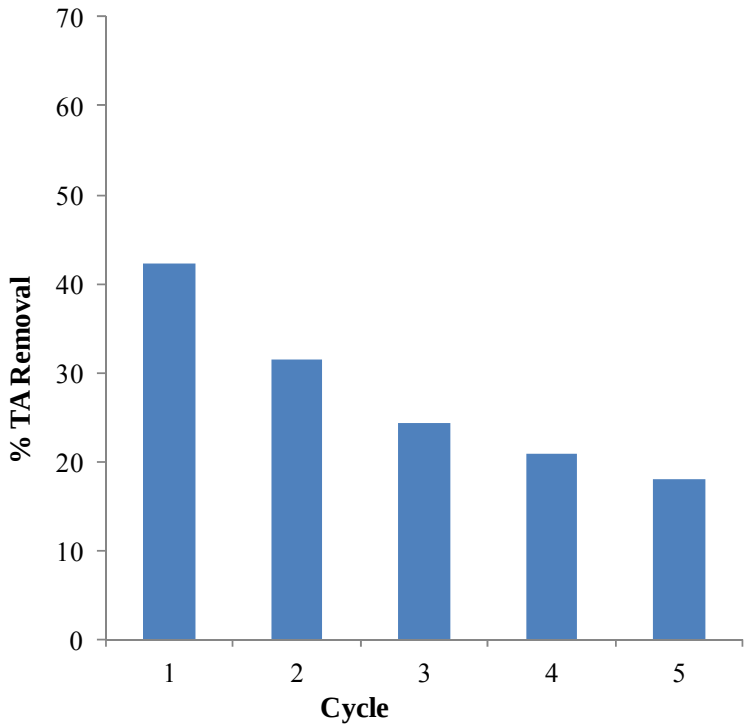

Figure 5.6c. TA removal efficiency of ACC after various desorption-adsorption cycles (with Ethanol).

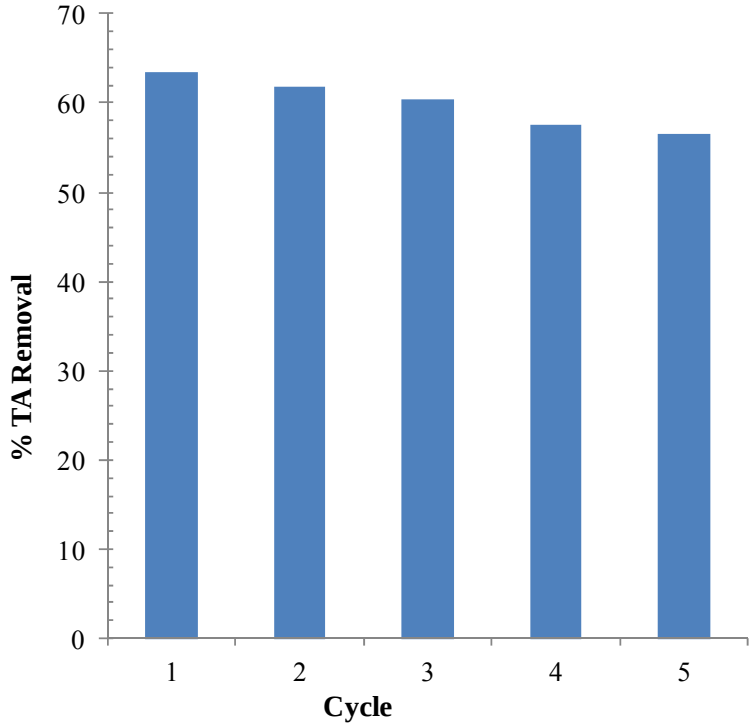

Figure 5.6d. TA removal efficiency of ACC after various thermal desorption-adsorption cycles.

CHAPTER- 6

CONCLUSIONS

On the basis of the results and discussion presented for the removal of TA from aqueous solution by adsorption process with ACC, following conclusions can be drawn:

- The BET surface area of ACC was found to be 222.33 m²/g, whereas the BET average pore diameter of ACC was 26.56 Å.
- Optimum conditions for the adsorptive treatment of TA by activated carbon-commercial grade (ACC) were found to be: initial pH ≈ 3, adsorbent dose of 15 g/l and contact time ≈7 h.
- Pseudo-second order kinetic model was found to fit the kinetic data.
- It was found that q_e values increases with increase in C_0, whereas, k_s decreases with an increase in C_0. Therefore, the uptake rate is limited by the C_0 of TA.
- Adsorption process was found to be endothermic in nature and Redlich–Peterson isotherm model was generally found to best represent the equilibrium data.
- Both surface and pore diffusion were found to be the rate-limiting steps in the adsorption process of TA onto ACC.
- Among various chemicals i.e. NaOH, ethanol and acetone, chemical desorption with acetone showed maximum desorption of TA from spent adsorbent. But, thermal desorption showed maximum desorption of TA from spent adsorbents.

REFERENCES

An, J.H., Dultz, S. 2007. "Adsorption of tannic acid on chitosan-montmorillonite as a function of pH and surface charge properties", Applied Clay Science 36, 256–264.

Aravindhan, R., Rao, J.R., Nair, B.U. 2007. "Removal of basic yellow dye from aqueous solution by adsorption on green algae Caulerpa scalpelliformis", Journal of Hazardous Material 142, 68–76.

Baker, F.S., Miller, C.E., Repik, A.J., Tolles, E.D. 1992. "Activated carbon", Kirk-Othmer Encyclopedia of Chemical Technology 4, 1015-1037.

Burdock G.A. 1997. "Encyclopedia of Food and Color Additives", Boca Raton: CRC.

Blanchard, G., Maunaye, M., Martin, G. 1984. "Removal of Heavy Metals from Water by Means of Natural Zeolites", Water Research 18, 1501-1507.

Chang, M.Y., Juang, R.S. 2004. "Adsorption of tannic acid, humic acid, and dyes from water using the composite of chitosan and activated clay", Journal of Colloid and Interface Science 278, 18–25.

Cheng, W., Dastgheib, S.A., Karanfil, T. 2005. "Adsorption of dissolved natural organic matter by modified activated carbons",Water Research 39, 2281–2290.

Food Chemicals Codex Committee. 1996. "Food Chemicals Codex", (4th ed.). Washington National Academy.

Figaro, S., Louis, S., Lambert, J., Ehrhardt, J.J., Ouensanga, A., Gaspard, S. 2006. "Adsorption studies of recalcitrant compounds of molasses spentwash on activated Carbons", Water Research 40, 3456–3466.

Freundlich, H.M.F. 1906. "Over the adsorption in solution", Journal of Physical Chemistry 57, 385-471.

He, P.J., Xue, J.E., Shao, L.M., Li, G.J. 2006. "Dissolved organic matter (DOM) in recycled leachate of bioreactor landfill", Water Research 40, 1465–1473.

Ho, Y.S., McKay, G. 1999. "Pseudo-second order model for adsorption processes", Process Biochemistry 34, 451-465.

Langmuir, I. 1918. “The adsorption of gases on plane surfaces of glass, mica and platinum”, Journal of American Chemical Society 40, 1361-1403.

Lin, C.F., Wu, C.H., Lai, H.T. 2008. “ Dissolved organic matter and arsenic removal with coupled chitosan/UF operation”, Separation Science Technology 60, 292–298.

Lin, J., Zhan, Y., Zhu, Z., Xing, Y. 2011. “Adsorption of tannic acid from aqueous solution onto surfactant-modified zeolite”, Journal of Hazardous Materials 193, 102– 111.

Mark, D., Williams., Pirbazari, M. 2007. “Membrane bioreactor process for removing biodegradable organic matter from water”, Water Research 41, 3880–3893.

Marquardt, D.W. 1963. An algorithm for least-squares estimation of nonlinear parameters. Journal of the Society for Industrial and Applied Mathematics 11, 431-44.

Mussatto, S.I., Roberto, I.C. 2001. “Hydrolysate detoxification with activated charcoal for xylitol product by Candida guilliermondii”, Biotechnology Letters 23, 1681-1684.

Rafatullaha, M., Sulaimana, O., Hashima, R., Ahmadb, A. 2010. “Adsorption of methylene blue on low-cost adsorbents: A review”, Journal of Hazardous Materials 177, 70–80.

Rauthula, M.S., Srivastava, V.C. 2011. Studies on adsorption/desorption of nitrobenzene and humic acid onto/from activated carbon. Chemical Engineering Journal 168, 35–43.

Redlich, O., Peterson, D.L. 1959. “A useful adsorption isotherm”, Journal of physical Chemistry 63, 1024-1026.

Ruthven, D. 1984. “Principles of Adsorption and Adsorption Processes”, Wiley Interscience.

Sharma, Y.C., Uma, Sinha, A.S.K., Upadhyay, S.N. 2010. “Characterization and Adsorption Studies of Cocos nucifera L. Activated Carbon for the Removal of

Methylene Blue from Aqueous Solutions", Journal of Chemical Engineering Data, 55, 2662–2667.

Srivastava, V.C., Swamy, M.M., Mall, I.D., Prasad, B., Mishra, I.M. 2006. "Adsorptive removal of phenol by bagasse fly ash and activated carbon: equilibrium, kinetics and thermodynamic study", Colloids and Surfaces, A: Physicochemical and Engineering Aspects 272, 89-104.

Srivastava, V.C., Mall, I.D., Mishra, I.M. 2007. "Adsorption thermodynamics and isosteric heat of adsorption of toxic metal ions onto bagasse fly ash (BFA) and rice husk ash (RHA)", Chemical Engineering Journal 132(1-3), 267-278.

Srivastava, A., Srivastava, V.C. 2009. "Adsorptive desulfurization by activated alumina", Journal of Hazardous Material 170(2-3), 1113-1140.

Suresh, S., Srivastava, V.C., Mishra, I.M. 2011. Isotherm, thermodynamics, desorption and disposal study for the adsorption of catechol and resorcinol onto granular activated carbon. Journal of Chemical Engineering Data 56(4), 811-818.

Suzuki, M., Fujii, T. 1982. "Concentration dependence of surface diffusion coefficient of propionic acid in activated carbon particles", AIChE Journal 28, 380-385.

Ucer, A., Uyanik, A., Cay S., Ozkan Y. 2005. "Immobilisation of tannic acid onto activated carbon to improve Fe(III) adsorption", Separation and Purification Technology 44, 11–17.

Ucer, A., Uyanik, A., Aygun, S.F. 2006. "Adsorption of Cu(II), Cd(II), Zn(II), Mn(II) and Fe(III) ions by tannic acid immobilised activated carbon", Separation and Purification Technology 47, 113–118.

Wang, J., Li, A., Xu, L., Zhou, Y. 2009. "Adsorption of tannic and gallic acids on a new polymeric adsorbent and the effect of Cu(II) on their removal", Journal of Hazardous Materials 169, 794–800.

Wang, J., Li, A., Xu, L., Zhou, Y. 2010. "Adsorption studies of tannic acid by commercial ester resin XAD-7", Chinese Journal of Polymer Science Vol. 28, No. 2, 231−239.

Wang, J., Zheng, S., Liu, J., Xu, Z. 2010. "Tannic acid adsorption on amino-functionalized magnetic mesoporous silica", Chemical Engineering Journal 165, 10–16.

Wang, J., Zheng, C., Ding, S., Ma, H., Ji, Y. 2011. "Behaviours and mechanisms of tannic acid adsorption on an amino-functionalized magnetic nanoadsorbent", Desalination 273, 285–291.

Zogorski, J.S., Faust, S.M., Hass, J.H. 1976. The kinetics adsorption of phenols by granular activated carbon. Journal of Colloid and Interface Science 55(2), 329-341.